Exp Brain Res (2003) 148:117–127
DOI 10.1007/s00221-002-1267-6

RESEARCH ARTICLE

Marianne Dieterich · Sandra Bense · Thomas Stephan · Tarek A. Yousry · Thomas Brandt

fMRI signal increases and decreases in cortical areas during small-field optokinetic stimulation and central fixation

Received: 30 October 2001 / Accepted: 30 August 2002 / Published online: 13 November 2002

Abstract Small-field optokinetic nystagmus (OKN) was performed in seven healthy volunteers in order to analyze the activation and deactivation patterns of visual motion, ocular motor, and multisensory vestibular cortex areas by means of fMRI during coherent visual motion stimulation. BOLD signal decreases (deactivations) were found in the first and second long insular gyri and retroinsular areas (the human homologue of the parietoinsular vestibular cortex and the visual posterior sylvian area in the monkey) of both hemispheres, extending into the transverse temporal gyrus and inferior-anterior parts of the superior temporal gyrus (BA 22), and the precentral gyri at two separate sites (BA 4 and 6). Further deactivations were found in cranioposterior parts of the superior temporal gyrus (BA 22) and the adjacent inferior parietal lobule (BA 40), anterior cingulate gyrus, hippocampus, and corpus callosum. Most of these BOLD signal decreases involved parts of the "multisensory vestibular cortical circuit". These findings support the concept of a reciprocally inhibitory visual–vestibular interaction that has now been demonstrated not only for large-field visual motion stimulation that induces vection (without eye movements) but also for optokinetically induced eye movements (without vection). The functional significance of this concept may be related to the perception of self-motion, since both large-field visual motion stimulation and optokinetic nystagmus are linked to the visual control of self-motion. With respect to activation of the cortical ocular motor system two separate and distinct areas of activations were delineated in the precentral sulcus of both hemispheres, one ventrolaterally (in BA 9) and the other dorsomedially at the junction of the superior frontal sulcus with the precentral sulcus (in BA 6). Both probably correspond to different subregions of the frontal eye field and the premotor cortex for the ocular motor performance of OKN.

Keywords Optokinetic nystagmus · Visual cortex · Vestibular cortex · Precentral gyrus · Functional MRI

M. Dieterich (✉) · S. Bense
Department of Neurology, Johannes Gutenberg University Mainz, Langenbeckstrasse 1, 55131 Mainz, Germany
e-mail: dieterich@neurologie.klinik.uni-mainz.de
Tel.: +49-6131-172510
Fax: +49-6131-175697

M. Dieterich · S. Bense · T. Stephan · T. Brandt
Department of Neurology, Klinikum Grosshadern, Ludwig-Maximilians University, Munich, Germany

T.A. Yousry
Department of Neuroradiology, Klinikum Grosshadern, Ludwig-Maximilians University, Munich, Germany

Introduction

In a previous functional magnetic resonance imaging (fMRI) study, we stimulated right-handed healthy volunteers with coherent visual pattern motion that induced optokinetic nystagmus (OKN) and found bilateral activation of the primary visual cortex and of visual motion-sensitive areas in the temporo-occipital cortex as well as ocular motor areas, for example, supplementary, frontal, and parietal eye fields, and the prefrontal cortex (Bucher et al. 1997; Dieterich et al. 1998). Furthermore, during this small-field optokinetic stimulation changes in BOLD signals were seen in the retroinsular and insular regions, where the human homologue of the parietoinsular vestibular cortex (PIVC) in monkeys is assumed to be located. In the only other brain activation study on OKN by using positron emission tomography (PET), Galati and co-workers (1999) also described activations of the visual areas, but they failed to show any significant signal changes in areas involved in the processing of ocular motor responses or vestibular information.

BOLD signal changes in the insular region including the PIVC during OKN became an interesting focus of research, since Grüsser and co-workers (1990a, b) first detected multisensory neurons in the PIVC in different monkey species which responded not only to vestibular stimuli but also to different somatosensory, visual, and optokinetic stimuli. Due to the close connections of this area with other multisensory areas receiving strong

vestibular input, such as areas 2v and 3aV, and strong visual input, such as area 7 and the visual temporal sylvian area, the authors called the PIVC the core region of a vestibular cortical circuit in the temporo-parieto-insular region (Guldin and Grüsser 1996).

Our current study focused on two questions: (A) is the vestibular cortex activated or deactivated during small-field OKN and (B) which cortical ocular motor areas are involved in the processing of small-field OKN?

A. In our earlier fMRI study we used radio frequency-spoiled single-slice fast low-angle shot (FLASH) pulse sequences with a specially developed data analysis to obtain a high spatial resolution (voxel size 0.78×0.78×4 mm; Bucher et al. 1997; Dieterich et al. 1998). This technique allowed measurements of signal changes but did not distinguish between BOLD signal increases and decreases. Therefore, the aim of the current fMRI study with echo-planar (echo-planar imaging; EPI) sequences was to analyze and to distinguish these activation and deactivation patterns during coherent visual motion stimulation in light of the interaction between visual motion, ocular motor, and multisensory vestibular cortex areas, especially in the PIVC in the posterior insula. This is of special interest because two contradictory results are theoretically possible: (1) signals in the PIVC could *increase* during optokinetic stimulation in humans, since PIVC neurons in monkeys responded to optokinetic stimulation (Grüsser et al. 1990a, b), and (2) signals in the PIVC could *decrease*, since an earlier PET activation study with large-field visual motion stimulation around the line of sight, which induced circular vection (but not OKN), showed deactivation of the PIVC and simultaneous activation of parieto-occipital visual areas (Brandt et al. 1998). The latter PET study concentrated on the cortical activation pattern during circular vection, whereas the current study concentrated on the effects of horizontal small-field visual optokinetic stimulation. This type of stimulation did not elicit apparent self-motion (no vection), but it did induce horizontal OKN. The question of whether the PIVC is activated or deactivated is functionally relevant for understanding the visual-vestibular cortical interactions that mediate the perception of self-motion. However, if the deactivation of the PIVC is combined with the perception of self-motion, it should not be induced during visual stimulation without vection.

B. There are two different gaze-stabilizing reflexes, the vestibulo-ocular and the optokinetic reflex (for review see Leigh and Zee 1999). In humans, the optokinetic response to a full-field moving visual stimulus has two phases, a slow phase depending on the visual stimulus and a quick phase resetting the eye (saccade). The slow phase consists of two components, the rapid *direct* component with a promptly generated nystagmus within 1–2 s of stimulus onset and the *indirect* component with a slower buildup of stored neural activity in the vestibular nuclei complex (Waespe and Henn 1987), the velocity-storage mechanism. When the light is switched off after sustained optokinetic stimulation, the nystagmus persists in the dark (i.e., optokinetic afternystagmus) due to the vestibular nucleus neurons, which continue discharging for some seconds (Cohen et al. 1977). They represent the velocity-storage mechanism. The slow build-up reflects not only the execution of optokinetic afternystagmus but also the perception of circular vection (Brandt and Dichgans 1972). It is suppressed by stationary objects in the peripheral visual field, whereas the rapid direct component does not reveal this property. The direct component is processed by premotor areas of the smooth pursuit eye movement system. This explains why deficits of OKN are usually combined with deficits of pursuit eye movements. Optokinetic stimulation with a small visual field and a rotating drum activates mainly the direct component linked to the smooth pursuit system.

The neuronal substrates important for the generation of OKN are located in the pretectum, which lies anterior to the superior colliculus between the mesencephalon and the posterior thalamus (for review see Ilg 1997). It includes the accessory optic system (AON) with three nuclei (dorsal, lateral, and medial terminal nucleus; DTN, LTN, MTN) and the nucleus of the optic tract (NOT) (Fuchs and Mustari 1993). Since NOT and DTN cannot be differentiated anatomically, they are discussed as an entity. The NOT and AON neurons receive not only retinal input but also input from neurons of the striate cortex and superior temporal sulcus (Hoffmann et al. 1991). Signals from NOT and AON travel in parallel to the nucleus prepositus hypoglossi and the vestibular nuclei complex, the neuronal substrate of the velocity-storage mechanism, and from there to the ocular motoneurons of the third, fourth, and sixth cranial nerves. Another projection from the NOT/DTN is directed to the ipsilateral dorsal cap of the inferior olive (Holstege and Collewijn 1982) and from there to the cerebellar nuclei. The finding of pursuit-related activity in NOT/DTN shows that there is some overlap in the neuronal substrate of OKN and pursuit eye movements. Further processing in the brainstem, however, seems to be different for each system: while the inferior olive is essential for OKN, the dorsolateral pontine nuclei are essential for pursuit eye movements. Neither system belongs to the brainstem centers responsible for the generation of saccades.

On the cortical level it is still not clear whether the neuronal substrate is identical or different for OKN and pursuit or whether the cortical eye centers overlap. Therefore, the question of which cortical ocular motor areas are involved in the processing of small-field OKN arises. This is of interest because two contradictory results are feasible: (1) activation patterns could be identical or similar to those known from earlier pursuit stimulation studies, since small-field OKN with a rotating drum generally induces the direct component, which is gener-

ated by areas that are also involved in the generation of pursuit eye movements or (2) the cortical activation pattern of OKN could, however, differ from that during pursuit, since recent brain activation studies comparing pursuit with saccade stimulation found separate and distinct subregions of cortical eye fields such as the frontal eye field (FEF; Petit and Haxby 1999). These data agree with FEF data using microstimulation in monkeys (Tian and Lynch 1996a, b). Thus, in view of the close anatomical connections of the OKN and the vestibular system, one could imagine that a separate and distinct subregion of the FEF is dedicated to the processing of optokinetic and vestibuloocular reflexes.

Materials and methods

Subjects

Seven right-handed healthy volunteers (three women, four men; mean age 26.6±3.5 years) without a history of visual, vestibular, or central nervous system disorders were examined. The local Ethics Committee of the Ludwig-Maximilians University of Munich approved the study, and all subjects gave their informed, written consent. The subjects were trained to perform ocular motor tasks.

Recording procedure and visual stimulation

Subjects lay supine wearing prism glasses, which allowed visual stimulation from outside the scanner. A rotating drum (diameter 0.4 m; constant rotation velocity 6–8°/s) covered with colored objects was placed in front of the MR scanner bore to elicit horizontal OKN. The field of view was restricted to 20° in the horizontal and 15° in the vertical dimensions, i.e., small-field stimulation that did not induce apparent self-motion (vection). The subjects were asked to report on the sensation of self-motion after the runs. The head was fixed by a head holder and the forehead was taped to the coil to reduce movement artifacts. Subjects had to fixate the drum during the whole fMRI acquisition, i.e., during the rest condition of 25 s when the subjects had to look straight ahead at a target in the center of the stationary drum and during the OKN stimulation conditions of 25 s for rightward or leftward OKN. Subjects were trained to perform horizontal OKN constantly over the whole stimulation period. This induced regular horizontal rightward or leftward OKN. During the rest condition eye movements were suppressed by fixation straight ahead. Under these conditions no optokinetic afternystagmus was elicited. Horizontal eye movements were recorded of both eyes with electrooculography (EOG) in two subjects to monitor task performance (for methods see Bucher et al. 1997). We recorded 140±20 beats/min during the OKN task and 2±2 beats/min during the fixation task (rest condition). The EOG recording thus demonstrated that the subjects were able to maintain OKN during the stimulation task and fixation during the rest condition. Slow-phase velocity was 6–8°/s during optokinetic stimulation conditions (i.e., a gain of 1 due to slow-velocity drum rotation).

Functional MRI acquisition

Functional images were acquired on a standard clinical scanner (Siemens Vision, Erlangen, Germany) at a magnetic field strength of 1.5 T, using a circularly polarized head coil and EPI with a T2*-weighted gradient-echo multislice sequence (TE=66 ms, TR=5,000 ms, voxel size 1.88×1.88×5 mm^3). Twenty transversal slices with a matrix size of 128×128 pixels covered the whole brain and the upper parts of the cerebellum. Each scanning session comprised two successive time series, one with OKN to the right and one with OKN to the left in randomized order. Each time series consisted of 60 images each. In both runs a block design of five images at rest and five images during stimulation was used; the first five images of each run were discarded because of spin saturation effects. During acquisition subjects lay supine with eyes open and wore an ear protection.

Data analysis

Data processing was performed on an UltraSPARC workstation (Sun Microsystems) using statistical parametric mapping (SPM96; Friston et al. 1995a) implemented in MATLAB (Mathworks, Natick, Mass., USA). All volumes were realigned to the first one of each scanning session to correct for subject motion, were spatially normalized (Friston et al. 1995b) into a standard stereotaxic space, using as template a representative brain from the Montreal Neurological Institute (MNI), and were compared to the stereotaxic atlas of Talairach and Tournoux (1988). Prior to statistical analysis, each image was smoothed with a 12-mm isotropic Gaussian kernel prior to statistical group analysis and a 6-mm isotropic Gaussian kernel prior to single subject analysis to compensate for intersubject gyral variability and to attenuate high frequency noise, thus increasing the signal to noise ratio. Statistical parametric maps were calculated on a voxel-by-voxel basis using the general linear model (Friston et al. 1995a) and the theory of Gaussian fields (Worsley and Friston 1995). SPM96 calculated the relative contributions of a delayed box car reference waveform as well as confounding variables (whole brain activity and low frequency variations) to the measured data. The delayed box car serves as a model of the expected hemodynamic response to the stimulus.

The results for relative BOLD signal increases (activations; contrast OKN – rest) were reported in accordance with an anatomically constrained hypothesis, since the aim of the study was to determine activations or deactivations of areas known from previous studies. Therefore, uncorrected P values were used (group: $P \leq 0.001$). As earlier studies showed that the activation pattern during OKN was independent of the horizontal stimulation direction (Bucher et al. 1997; Dieterich et al. 1998), the data for this group analysis were pooled for rightward and leftward optokinetic stimulation.

Task-induced BOLD MRI signal decreases (contrast rest – OKN) were also measured, but their significance is still not clearly understood. According to studies supporting the view that signal decreases in fMRI correlate with regional cerebral blood flow decreases in PET (Rauch et al. 1998; Fransson et al. 1999; Hutchinson et al. 1999), BOLD signal decreases may reflect functional deactivation. However, this correlation does not yet allow a conclusive statement about the neuronal activity in these areas. Consequently we analyzed this contrast rest – OKN without an a priori hypothesis and considered only P values corrected for multiple comparisons as significant (P=0.0001). For simplicity, we will at times use the term "deactivations" when referring to BOLD signal decreases.

Anatomical localization

To define the anatomical sites of activation and deactivation clusters derived by the different statistical approaches, we used the MNI coordinates as well as defined anatomical landmarks (Naidich et al. 1995; Naidich and Brightbill 1996; Stephan et al. 1997; Yousry et al. 1997) and the atlas of Talairach and Tournoux (1988).

To the best of our knowledge, there is still no internationally agreed upon definition of insular and retroinsular regions available in the literature. The insula was anatomically divided into five gyri, three short (I–III) and two long insular gyri (IV, V) (Bense et al. 2001). We defined the region anterior to the central insular sulcus as the anterior insula and it includes the short insular gyri (I–III). The region posterior to the central insular sulcus was defined as the posterior insula and it includes the first (IV) and second (V) long

Table 1 Areas with signal increases and signal decreases during small-field visual optokinetic stimulation obtained by statistical group analysis (n=7). Z-scores, corresponding Brodmann areas (*BA*), Montreal Neurological Institute coordinates (*X/Y/Z*), and cluster sizes (in voxel) of the signal maxima are given. Italics represent areas at lower significance levels, i.e., decreases of P=0.001, corrected, instead of P=0.0001, corrected. (*IV,V* Long insular gyri IV and V, *SPL* superior parietal lobule, *GTm* medial temporal gyrus, *GTs* superior temporal gyrus)

Z-score	Area	R/L	BA	X	Y	Z	Cluster
Signal increases: activations (P=0.001 uncorrected)							
8.55	Lingual gyrus	L	18	–6	–86	–4	17,969
8.21	Cuneus	R	18	24	–96	6	
8.16	Cuneus/medial occipital gyrus	L	18	–24	–94	18	
6.73	Precuneus	R	7	20	–62	64	827
4.58	Precentral gyrus	L	6	–44	0	56	116
4.49	Precentral gyrus	R	9	50	8	42	105
4.36	Precentral gyrus	R	6	30	0	62	81
4.25	Precuneus/SPL	L	7	–26	–54	64	175
3.46	*Precentral gyrus*	*L*	*9*	*–60*	*6*	*38*	*50*
Signal decreases: deactivations (P=0.0001, corrected)							
6.74	Posterior corpus callosum/white matter	L		–16	–46	20	2,607
5.56	White matter of GTm	R		30	–48	26	
5.27	Posterior cingulum	R	29/23	16	–48	22	
6.26	Posterior insula (IV, V), GTs	R	(IV/V)/22	40	–16	8	2,380
5.20	Hippocampus	R	(E3)	28	–20	–14	
4.86	Hippocampus	R	28 (E2)	30	–10	–18	
5.64	Posterior insula (IV, V)	L	IV,V/6	–44	–12	16	845
				–44	–16	0	
4.68	Anterior corpus callosum	R	24	8	22	18	957
4.59	Anterior corpus callosum	L	24	–10	22	18	
4.44	Anterior cingulate gyrus	L	24/32	–4	40	8	
4.40	Medial frontal gyrus	R	11	16	36	–18	82
4.07	Medial frontal gyrus	R	11	16	26	–24	
4.25	Inferior frontal gyrus	R	47	22	8	–18	117
4.11	Inferior anterior insula	R		28	16	–12	
4.18	Precentral gyrus	R	4	20	–24	54	82
4.05	*Precentral gyrus*	*L*	*6*	*–2*	*–18*	*62*	
3.53	*Precentral gyrus*	*L*	*4*	*–34*	*–18*	*56*	

insular gyri. The retroinsular territory was defined as the area posterior to the second long insular gyrus.

Results

None of the healthy volunteers reported apparent self-motion (vection). For better reading of the Results section we will indicate the sites of the BOLD signal increases and decreases in the form of gyri and lobes. The exact anatomical location is given in MNI coordinates and Brodmann areas (BA) in Table 1.

BOLD signal increases of the visual cortex and ocular motor areas

Visual optokinetic stimulation in both horizontal directions within a restricted field of view caused bilateral BOLD signal increases of the striate and extrastriate visual cortex areas. The maximum activation occurred in the lingual gyrus, inferior and medial occipital gyri, inferior temporal gyrus, cuneus (BA 18, 19), and in the temporo-parieto-occipital area of the medial temporal gyrus including V5 (Table 1; Fig. 1). The bilateral parieto-occipital clusters of activation extended from the visual cortex to the occipital gyrus (BA 19) and to the precuneus (BA 7), more so on the right than on the left, and into the adjacent left superior parietal lobule. Significant increases were further found in the precentral gyri in both hemispheres at two different sites, one in the dorsal and medial parts (BA 6) at the junction of the superior frontal sulcus with the precentral sulcus, and the other in ventral and lateral parts (BA 9) at the border to the medial frontal gyrus (Fig. 1). The activation at BA 9 was significant in the right hemisphere at a P=0.001 level and in the left hemisphere at a P=0.01 level.

BOLD signal decreases of posterior insular and retroinsular cortex areas

Negative BOLD MRI responses were calculated for both optokinetic stimulation directions (P=0.0001, corrected for multiple comparisons). Large signal decreases in the temporo-parietal lobe of both hemispheres extended continuously from the posterior insula (first and second long insular gyri), retroinsular areas, the transverse temporal gyri (BA 41), and superior temporal gyri (BA 22) to the pre- and postcentral gyri (BA 4 and 6) (Fig. 2). Signal decreases in insular and retroinsular regions appeared to be larger in the right hemisphere (2,380 voxels, Z-score 6.26 vs 845 voxels, Z-score 5.64; Table 1) and were located around –10 and +10 for the z-coordinate as shown in the single subject analysis (mean coordinates, right hemisphere, $x/y/z$=+42/–13/+0.5, left hemisphere $x/y/z$=–48/–11/+0.7; Table 2). In the group analysis the z-coordinates gave a more dorsal localization (right: $x/y/z$=+40/–16/+8; left: $x/y/z$=–44/–12/+16 and

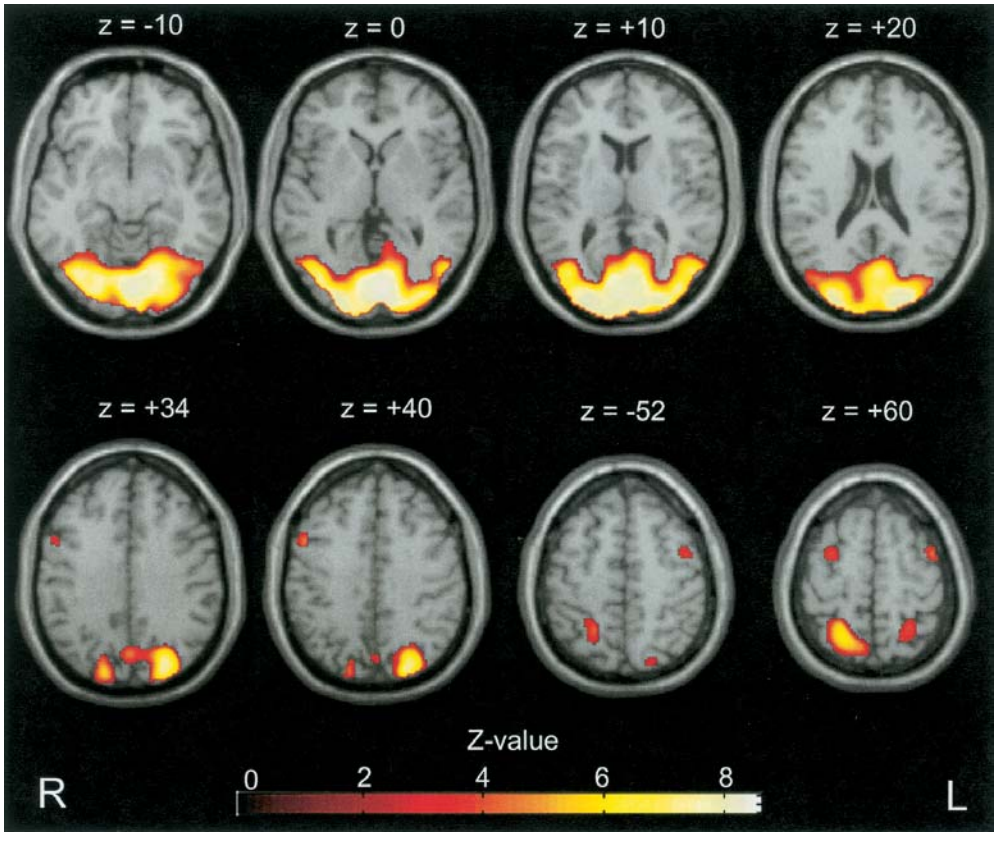

Fig. 1 Activation areas during horizontal visual optokinetic stimulation of a restricted field of view obtained by statistical group analysis (n=7). Activation maps were superimposed onto selected transverse sections of a standard brain template and thresholded at P=0.001 (uncorrected). Activations were found bilaterally in the striate and extrastriate visual cortex areas with the maximum in the lingual gyrus, inferior and medial occipital gyri, inferior temporal gyrus, cuneus, as well as in the temporo-occipital areas, the occipital gyrus, and the precuneus. In addition, significant increases were found in the precentral gyri in both hemispheres at two different sites, one in the rostral and medial parts (BA 6) at the junction of the superior frontal sulcus with the precentral sulcus and the other in caudal and lateral parts (BA 9) at the border to the medial frontal gyrus. The corresponding Montreal Neurological Institute (MNI) coordinates and Z-scores are listed in Table 1

–44/–16/0) because the clusters of signal decreases were not as discrete as in the single subjects but formed a continuum extending to temporal and inferior parietal regions.

Additional signal decreases were found in more superior and occipital parts of the superior temporal gyri (BA 22) in the right hemisphere reaching into the inferior parietal lobule (BA 40) as well as bilaterally into the hippocampus, the adjacent optic radiation, the corpus callosum, and the anterior cingulate gyri (BA 24, 32). Other signal decreases were seen in the right hemisphere in the inferior (BA 47) and medial frontal gyrus (BA 11), and the inferior parts of the anterior insula. In dorsal brain regions signal decreases of the precentral gyrus extended into two Brodmann areas, bilaterally in BA 4 and on the left side in BA 6 (visible with P=0.001).

Table 2 Montreal Neurological Institute coordinates of signal decreases of the insular region during small-field visual optokinetic stimulation obtained by single subject analysis (n=7). – No signal decrease in the insular region

Subject	Right			Left		
	X	Y	Z	X	Y	Z
1	+42	–18	+4	–48	–8	+4
2	+46	–12	–2	–46	–16	+10
3	–	–	–	–50	–22	–6
4	+40	–12	–6	–50	–4	–6
5	–	–	–	–52	–4	0
6	+40	–10	+6	–42	–14	+2
7	–	–	–	–	–	–
Mean	+42	–13	+0.5	–48	–11	+0.7
Range						
From	+40	–18	–6	–42	–22	–6
To	+46	–10	+6	–52	–4	+10

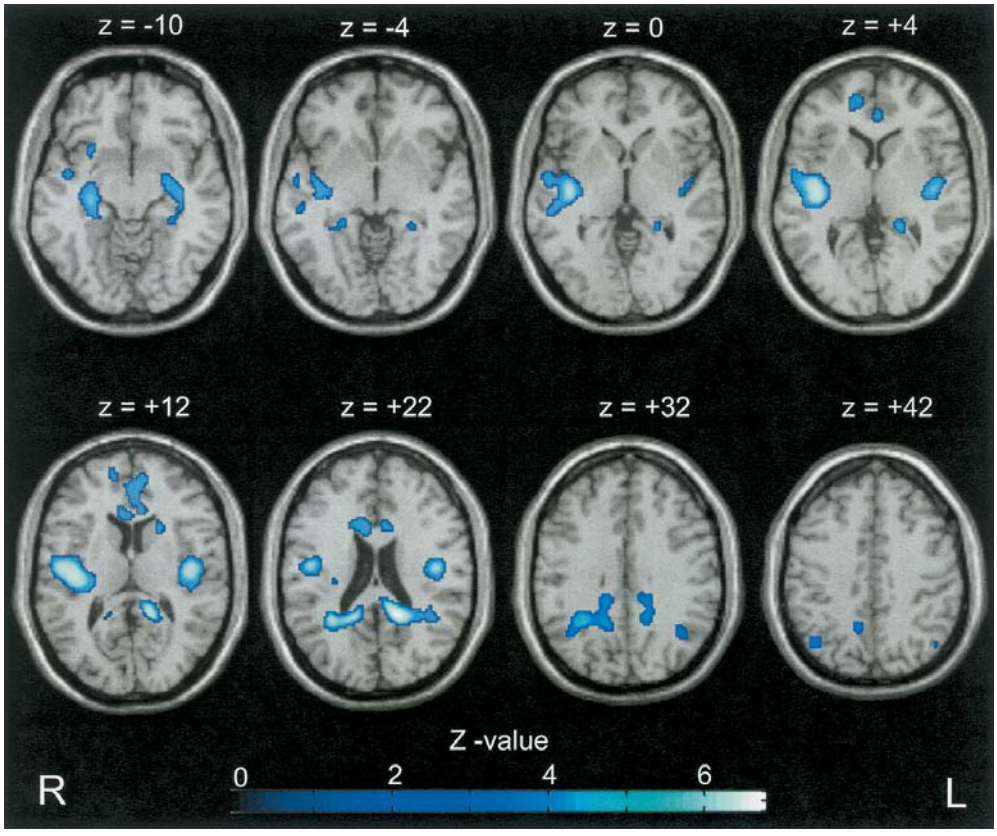

Fig. 2 Areas with signal decreases during visual optokinetic stimulation of a restricted field of view obtained by statistical group analysis (n=7). Activation maps were superimposed onto selected transverse sections of a standard brain template and thresholded at P=0.0001, corrected for multiple comparisons. Signal decreases were found in clusters of the temporo-parietal lobe bilaterally, including the posterior insula (first and second long insular gyri), retroinsular areas, the transverse temporal gyri (BA 41), superior temporal gyri (BA 22), and pre- and postcentral gyri (BA 4 and 6). Additional signal decreases were seen in rostrodorsal parts of the superior temporal gyri (BA 22) in the right hemisphere, reaching into the inferior parietal lobule (BA 40), the inferior-anterior insula, as well as bilaterally in the hippocampus with the adjacent optic radiation, the corpus callosum, and the anterior cingulate gyri (BA 24, 22). In the rostral brain regions signal decreases of the precentral gyrus extended into two Brodmann areas, bilaterally into BA 4 and on the left side into BA 6 (not mapped). The corresponding MNI coordinates and Z-scores are listed in Table 1

Discussion

BOLD signal increases: activations

Small-field optokinetic stimulation inducing horizontal optokinetic nystagmus caused a bilateral BOLD signal increase of visual cortex areas such as the primary visual cortex (BA 18, 19), the motion-sensitive areas at the junction of occipital and temporal cortex in the medial temporal gyrus [medial temporal/medial superior temporal (MT/MST) areas; MT/V5], and areas in the parieto-occipital cortex with the occipital gyrus (BA 19) and the precuneus (BA 7). These activations of the visual system agreed closely with the data of earlier PET and fMRI studies on visual stimulation (Zeki et al. 1991; Barton et al. 1996; Goebel et al. 1998; Sunaert et al. 1999).

Furthermore, cortical ocular motor centers such as the FEF were bilaterally activated. This effect of OKN thus confirms the two earlier fMRI studies on OKN done with FLASH pulse sequences (Bucher et al. 1997; Dieterich et al. 1998). For the first time we were now able to differentiate two separate activation loci in the precentral gyrus of both hemispheres: one was inferior-lateral in BA 9 and the other anteromedial at the junction of the superior frontal sulcus with the precentral sulcus in BA 6. The question arises whether they can both be attributed to the FEF or to the FEF and a premotor cortex area associated to the FEF. Up to now FEF activation in functional brain imaging studies has been examined during saccades or smooth pursuit eye movements, not during OKN. In several studies with PET and fMRI, the human FEF subserving visually guided saccades was located in the precentral cortex in BA 6, unlike the monkey FEF, which was located in the posterior part of BA 8. Comparing FEF activation during smooth pursuit and saccades, Petit and Haxby (1999) localized the site in the precentral gyrus, with a mean location of pursuit-related activity most often inferior and lateral to the saccade-related activity ($x/y/z$=36±5/–10±4/47±3 for saccades and 44±4/–7±4/43±3 for pursuit in the right

hemisphere). This anatomical localization corresponded to the human FEF identified earlier for different types of saccades (for review see Paus 1996; Petit et al. 1997; Luna et al. 1998) and to microstimulation studies in monkeys (Gottlieb et al. 1993, 1994; Tian and Lynch 1996a, b). Several subregions that were separate and distinct for pursuit and saccades have also been delineated in most of the cortical eye fields in monkeys by using microstimulation (Tian and Lynch 1996a, b). For example, the monkey FEF has an area in the rostral bank of the arcuate sulcus that controls saccades, and a more posterior subregion in the arcuate sulcus that controls pursuit (Gottlieb et al. 1993, 1994; Tian and Lynch 1996a, b). However, the locations of these FEF subregions during saccades and pursuit in humans (Petit and Haxby 1999) both do not exactly agree with our data, since one of our activity sites was markedly more inferior, anterior, and lateral (+50/+8/+42 in BA 9) and the other slightly more superior at the junction with the superior frontal sulcus (+30/0/+62 or +44/0/+56 in BA 6). Whereas the latter came close to the FEF activation described earlier during saccades (Paus 1996; Luna et al. 1998), activity peaks of the first were especially more lateral and inferior to the second, which was located at the border to the medial frontal gyrus.

The FEF localization in the literature is remarkably consistent across all saccade studies for the dorsal-ventral and anterior-posterior directions; the mediolateral position may vary considerably, probably due to the type of ocular motor task (Paus 1996). However, the localization of our activations differs in all three directions, especially in the dorsal-ventral direction. If the location of our two activations is valid, our study might provide evidence for further subregions in the human FEF, not only the two known from the literature to be related to the execution of smooth pursuit and saccadic eye movements, but also for an additional one, probably related to OKN (in BA 6).

Optokinetic nystagmus could be simply defined as an eye movement that combines the initial response of a smooth pursuit component with a large resetting saccade. This simplified definition would lead us to expect FEF activity in both the pursuit-related and the saccade-related subregions. However, this was not the case in our study. We found two activation sites, but neither corresponded exactly to earlier data for pursuit or saccade subregions of FEF. Especially the location of FEF related to smooth pursuit did not fit, although the small-field OKN stimulus with a rotating drum is believed to preferably induce pursuit eye movements related to the rapid direct component of OKN (and not the indirect component of OKN). Indeed, studies on monkeys have provided evidence of a more complex system related to optokinetic stimulation, the *vestibular-optokinetic* system (Leigh and Zee 1999). It seems to be responsible for especially the indirect component of OKN, i.e., the slower build-up related to the vestibular nuclei complex. The close connection between the vestibular and optokinetic systems is demonstrated by vestibular nucleus neurons that responded to monkey head rotations and were also driven by optokinetic stimuli (Boyle et al. 1985), or continued discharging for some seconds when the lights were turned off after a period of optokinetic stimulation (Waespe and Henn 1977). The vestibular-optokinetic system probably also influences the cortical activation pattern during small-field OKN, which would explain why the FEF activation did not correspond to the expected FEF activation located at the site of the pursuit subregion.

In view of these differences in FEF localization, the question arises if there is also a partly independent, different ocular motor network for OKN at the cortical level with separate subregions in the cortical eye fields such as FEF, supplementary eye field (SEF), and parietal eye field (PEF). Current fMRI research (Petit and Haxby 1999) provides evidence for the hypothesis, based on the results of monkey experiments (Tian and Lynch 1996a, b), that two parallel corticocortical systems mediate the control of eye movements; one of these systems controls visually guided saccades and the other controls visual pursuit. Both systems in the monkey are composed of several interconnected subregions, distributed across different cortical eye fields such as the FEF, SEF, PEF, and MT/MST, and dorsomedial parietal visual areas. Within each of these cortical eye fields, one group of neurons serves as a subregion in the network and is solely devoted to saccadic eye movements, and a second group, which generally does not overlap with the first, serves as a subregion solely devoted to pursuit eye movements (Tian and Lynch 1996a, b). In healthy humans the network is composed of the same areas as in the monkey, FEF, SEF, PEF, and MT/MST (Müri et al. 1996; Petit et al. 1997; Luna et al. 1998), as well as an additional area, the medial cortical region of the precuneus (Luna et al. 1998; Petit and Haxby 1999). The latter was also activated in our study during OKN. The probable homologue in monkeys, an area in the medial wall of the posterior parietal lobe (consisting of area 7m and the dorsomedial visual area), is involved in ocular motor control (Cavada and Goldman-Rakic 1989a, b; Tian and Lynch 1996b) and the transmission of visual motion information from the visual cortex to the FEF (Tian and Lynch 1996b). In cats unilateral lesions of the middle suprasylvian cortex involving area 7 and the lateral suprasylvian area, comparable with parts of the parietal area 7 in humans and monkeys, induced a decrease in ipsilateral slow-phase velocity of OKN (Ventre 1985) similar to that reported in monkeys (Lynch and McLaren 1983). These parietal areas in the cat project ipsilaterally to the NOT and AON, the ocular motor nuclei in the brainstem responsible for the generation of OKN (Ventre 1985).

Our data also seem to provide first evidence of a second OKN-related subregion (in BA 9) in the precentral gyrus, inferior-lateral to the first, that may represent a premotor cortex area related to optokinetic eye movements. A premotor cortex area with a similar localization was recently described for saccades (Heide et al. 2001). This finding and the finding of a probable OKN-related subregion of the FEF have to be confirmed in further visuomotor studies on OKN. This is necessary since, as

mentioned before, the only other study available so far on OKN by Galati and co-workers (1999) done with PET failed to show any significant signal changes in areas involved in the processing of ocular motor responses or vestibular information during OKN. This might be due to the technique of PET.

BOLD signal decreases: deactivations

Vestibular neurons of monkeys respond well to only low-frequency visual stimuli. This finding is in accordance with the demands made on the optokinetic system to support the vestibuloocular reflex during sustained rotation (Leigh and Zee 1999). Only when vestibular and optokinetic stimulation are combined, as during the natural situation of self-rotation, the optokinetic input takes over as the vestibular drive declines at constant velocity and maintains a steady vestibular discharge that continues to generate compensatory eye movements. The above-described close, functional cooperation of the optokinetic and the vestibular systems, known from the physiology and neuroanatomy of animal studies, allows us to explain the following findings within the multisensory vestibular cortex areas in humans during stimulation of only the visual optokinetic system (without stimulation of the vestibular system).

The most interesting findings were the locations of the relative BOLD signal decreases. These were observed in the posterior insula of both hemispheres involving the first and second long insular gyri (gyri IV and V) and retroinsular territories, the anterior cingulate gyrus (BA 24), the precentral gyrus at two sites (BA 4 and BA 6), the hippocampus, and the corpus callosum. The site in the posterior insula corresponded well to the location of rCBF decreases found in PET during torsional full-field visual stimulation without OKN which induced the sensation of self-motion, i.e., circular vection (Brandt et al. 1998). However, the horizontal visual stimulation in the current study was restricted to a small field of view, which did not elicit circular vection. Thus, the signal decrease under this stimulation condition was not induced by the sensation of self-motion, but rather by the small-field motion stimulation or, which is more likely, the optokinetic eye movement. Indeed, the OKN-induced signal changes in the posterior insula were not seen if OKN was suppressed by a stationary target during motion stimulation (fixation suppression of OKN; fMRI: Dieterich et al. 1998; PET: Bense et al. 2002).

These insular regions were described by Grüsser and co-workers (1990a, b; Guldin and Grüsser 1996) as being located "in the upper bank of the lateral sulcus around the posterior end of the insula, sometimes also within the upper posterior end of the insula". The neurons in these regions, called neurons of the PIVC in different monkey species, were multisensory and responded not only to vestibular and somatosensory stimulations but also to optokinetic stimulation. The preferred direction of optokinetic stimulation was not related to gravitational but rather to head coordinates (Grüsser et al. 1990b). When different (conflicting or enhancing) combinations of optokinetic and vestibular stimulation were used, no generalized type of interaction was observed. Of the PIVC neurons also responsive to a horizontally moving striped pattern (different constant angular velocities of 10–20 cm/s), 66% were activated if visual motion was opposite in direction to body acceleration, about 30% were activated by both stimuli optokinetic and vestibular in the same direction, and about 4% were biphasic (Grüsser et al. 1990b). Increasing neuronal impulse rates were observed with increasing velocities (up to about 60°/s), and the discharge patterns of these PIVC neurons were not correlated to saccades. The neurons were also activated by a stimulation of a very small visual field (visual eye tracking of a small light stimulus); however, the most effective stimulus was the movement of a large, structured visual pattern (more than 30° of the visual field) in an optimal direction that induced OKN (Grüsser et al. 1990a, b).

The area of BOLD signal decreases in our study extended into the retroinsular region, the superior temporal gyrus, and the adjacent inferior parietal lobule. In a region adjoining the PIVC at its posterior border, Grüsser and co-workers frequently recorded action potentials of "purely" visual neurons, which either did not respond to vestibular or somatosensory stimuli at all (Grüsser et al. 1990a, b) or were driven or modulated by vestibular stimuli in only 30% of the neurons (Guldin and Grüsser 1998). This retroinsular region, termed the visual temporal sylvian area or the visual posterior sylvian area (VPS; Guldin and Grüsser 1996, 1998), appeared to also be deactivated in our study.

In earlier PET and fMRI studies using vestibular caloric (Dieterich et al. 1999) and vestibular galvanic (Bucher et al. 1998; Bense et al. 2001) stimulation, posterior insular areas were bilaterally activated and identified as the human homologue of the monkey PIVC. The latter imaging studies in humans localized PIVC around the bicommissural line of Talairach (AC-PC) at a level between –10 and +10 mm along the *z*-axis (for example, activations during galvanic vestibular stimulation: *x*/*y*/*z*=+43/–16/+11; Bense et al. 2001). The coordinates of those activations were similar to those of the deactivations in the posterior insula found in our study (*x*/*y*/*z*=+40/–16/+8). These findings give evidence: (a) that the area in the posterior insula represents the human homologue of the PIVC in the monkey and (b) that the human PIVC can show BOLD signal or rCBF increases during vestibular stimulation and BOLD signal or rCBF decreases during small-field OKN and large-field visual stimulation.

The only other study on vestibular galvanic stimulation using EPI sequences attributed the PIVC to an activation area in the temporo-parietal junction 20 mm above the AC-PC level (*x*/*y*/*z*=–64/–36/+20; Lobel et al. 1998). These coordinates, however, correspond better to lower parts of the inferior parietal lobule (BA 40 bordering BA 22), which we attribute to monkey area 7 and not to

PIVC (Bense et al. 2001). Other clusters of deactivations in the current study were concentrated in these rostral-dorsal parts of the superior temporal gyrus (BA 22 bordering BA 40) and the adjacent lower parts of the inferior parietal lobule (BA 40) at the temporo-parieto-occipital junction (Fig. 2). The inferior parietal lobule most likely represents the multisensory area 7 of the monkey, where the neurons discharge during both stimuli, rarely during vestibular stimulation, and regularly during visual optokinetic stimulation (Kawano et al. 1980; Andersen 1987; Faugier-Grimaud and Ventre 1989; Guldin and Grüsser 1998). Areas 7a and 7b as well as area VPS are closely interconnected with the PIVC and correspond to parts of the multisensory corticovestibular system ("inner vestibular circle") in monkeys as postulated by Guldin and Grüsser (1996, 1998). In our study, all these multisensory vestibular cortex areas appeared deactivated. Further deactivations were found during OKN in the anterior cingulate gyri, the hippocampus, and the precentral gyrus (BA 4 and 6). The posterior arcuate area in monkeys (area 6pa) is part of the premotor area 6, which sends efferent axons to the vestibular nuclei as well as to the PIVC. Areas in the cingulate sulcus, hippocampus, and area 6 also belong to the multisensory vestibular cortical circuit (Guldin and Grüsser 1996, 1998). Conversely, stimulation of the human vestibular system by caloric and galvanic irrigation of the vestibular nerve was associated with significant activations in most of these areas, especially in the hippocampus (Bottini et al. 1994; Vitte et al. 1996; Lobel et al. 1998; Bense et al. 2001).

Why are there BOLD signal decreases in the vestibular cortex during OKN?

The activation–deactivation pattern found during visual optokinetic stimulation confirms the recent finding of a reciprocally inhibitory interaction between the visual (here optokinetic) and the vestibular systems. This interaction between the two systems was first described in a PET study during large-field visual stimulation with circular vection but without optokinetic eye movements (Brandt et al. 1998). Activations of visual cortex areas were combined with regional blood flow decreases of the PIVC, a finding confirmed by Kleinschmidt and co-workers (2002) in fMRI. It was hypothesized that these inhibitory visual–vestibular interactions have a functional significance, i.e., that a potential mismatch between two incongruent or misleading sensory inputs is suppressed owing to the sensorial weight being shifted to the dominant or more reliable modality (Brandt et al. 1998). BOLD signal decreases of the PIVC in the current study were most likely induced by optokinetic eye movements rather than by purely visual motion stimulation input, since modulation of PIVC activity was not seen during fixation suppression of OKN (Dieterich et al. 1998; Bense et al. 2002). However, large-field visual motion stimulation and small-field optokinetic stimulation have in common that they are both linked to the visual control of self-motion.

Those multisensory vestibular cortex areas that showed signal *decreases* in the current study typically exhibited signal *increases* during vestibular stimulation, such as caloric (Bottini et al. 1994; Vitte et al. 1996) or galvanic excitation (Lobel et al. 1998; Bense et al. 2001) of the vestibular nerve. Conversely, when the vestibular system was activated, deactivations of the visual system were found (Wenzel et al. 1996). Vestibular caloric stimulation in PET showed that an activation of the multisensory vestibular cortex in the posterior insula (PIVC) was accompanied by a simultaneous decrease of the rCBF of the entire visual cortex bilaterally, covering BA 17, 18, and 19. This holds not only for visual–vestibular and vestibular–visual interactions but also for an inhibitory nociceptive–somatosensory interaction (Bense et al. 2001). Thus, the mode of interaction between the visual, optokinetic, vestibular, nociceptive, and somatosensory systems depends on the actual inter-sensory stimulation condition.

Acknowledgements We are grateful to Judy Benson for critically reading the manuscript. This work was supported by the Deutsche Forschungsgemeinschaft (BR 639/5–3; DI 379/4–1), the Wilhelm-Sander-Stiftung, and the Stifterverband.

References

Andersen RA (1987) Inferior parietal lobule function in spatial perception and visuomotor integration. In: Mountcastle VB, Plum F, Geiger SR (eds) Handbook of physiology, sect I. The nervous system, vol V. American Physiological Society, Bethesda, pp 483–518

Barton JJ, Simpson T, Kiriakopoulos E, Steward C, Crawley A, Gutrie B, et al (1996) Functional MRI of lateral occipitotemporal cortex during pursuit and motion perception. Ann Neurol 40:387–398

Bense S, Stephan T, Yousry TA, Brandt T, Dieterich M (2001) Multisensory cortical signal increases and decreases during vestibular galvanic stimulation (fMRI). J Neurophysiol 85:886–899

Bense S, Stephan T, Bartenstein P, Schwaiger M, Brandt T, Dieterich M (2002) Optokinetic stimulation and its fixation suppression (PET study). J Neurol 249(suppl 1):25

Bottini G, Sterzi R, Paulescu E, et al (1994) Identification of the central vestibular projection in man: a positron emission tomography activation study. Exp Brain Res 99:164–169

Boyle R, Büttner U, Markert G (1985) Vestibular nuclei activity and eye movements in the alert monkey during sinusoidal optokinetic stimulation. Exp Brain Res 57:362–369

Brandt T, Dichgans J (1972) Circularvection, optische Pseudocorioliseffekte und optokinetischer Nachnystagmus. Albrecht von Graefes Arch Ophthalmol 184:42–57

Brandt T, Bartenstein P, Janek A, Dieterich M (1998) Reciprocal inhibitory visual-vestibular interaction: visual motion stimulation deactivates the parieto-insular vestibular cortex. Brain 121:1749–1758

Bucher SF, Dieterich M, Seelos KC, Brandt T (1997) Sensorimotor cerebral activation during optokinetic nystagmus. A functional MRI study. Neurology 49:1370–1377

Bucher SF, Dieterich M, Wiesmann M, Weiss A, Zink R, Yousry TA, Brandt T (1998) Cerebral functional magnetic resonance imaging of vestibular, auditory, and nociceptive areas during galvanic stimulation. Ann Neurol 44:120–125

Cavada C, Goldman-Rakic PS (1989a) Posterior parietal cortex in rhesus monkey. 2. Evidence for segregated cortico-cortical networks linking sensory and limbic areas with the frontal lobe. J Comp Neurol 287:422–445

Cavada C, Goldman-Rakic PS (1989b) Posterior parietal cortex in rhesus monkey. 1. Parcellation of areas based on distinctive limbic and sensory corticocortical connections. J Comp Neurol 287:393–421

Cohen B, Matsuo V, Raphan T (1977) Quantitative analysis of the velocity characteristics of optokinetic nystagmus and optokinetic after-nystagmus. J Physiol 270:321–344

Dieterich M, Bucher SF, Seelos KC, Brandt T (1998) Horizontal or vertical optokinetic stimulation activates visual motion-sensitive, ocular motor and vestibular cortex areas with right hemispheric dominance. An fMRI study. Brain 121:1479–1495

Dieterich M, Bense S, Brandt T, Schwaiger M, Bartenstein P (1999) Dominance of the non-dominant hemisphere for processing vestibular information (PET study). Neuroimage 6:499

Faugier-Grimaud S, Ventre J (1989) Anatomic connections of inferior parietal cortex (area 7) with subcortical structures related to vestibulo-ocular function in monkey (*Macaca fascicularis*). J Comp Neurol 280:1–14

Fransson P, Krüger G, Merboldt KD, Frahm J (1999) MRI of functional deactivation: temporal and spatial characteristics of oxygenation-sensitive responses in human visual cortex. Neuroimage 9:611–618

Friston KJ, Holms AP, Worsley KJ, Poline JB, Frith CD, Frackowiak RSJ (1995a) Statistical parametric maps in functional imaging: a general linear approach. Hum Brain Map 2:189–210

Friston KJ, Asburner J, Frith CD, Poline JB, Heather JD, Frackowiak RSJ (1995b) Spatial registration and normalization of images. Hum Brain Map 2:165–189

Fuchs A, Mustari M (1993) The optokinetic response in primates and its possible neuronal substrate. In: Miles F, Wallman J (eds) Visual motion and its role in the stabilization of gaze. Elsevier, Amsterdam, pp 343–349

Galati G, Pappata S, Pantano P, Lenzi GL, Samson Y, Pizzamiglio L (1999) Cortical control of optokinetic nystagmus in humans: a positron emission tomography study. Exp Brain Res 126:149–159

Goebel R, Khorram-Sefat D, Muckli L, Hacker H, Singer W (1998) The constructive nature of vision: direct evidence from functional magnetic resonance imaging studies of apparent motion and motion imagery. Eur J Neurosci 10:1563–1573

Gottlieb JP, Bruce CJ, McAvoy MG (1993) Smooth eye movements elicited by microstimulation in the primate frontal eye field. J Neurophysiol 69:786–799

Gottlieb JP, McAvoy MG, Bruce CJ (1994) Neural responses related to smooth-pursuit eye movements and their correspondence with electrically elicited smooth eye movements in the primate frontal eye field. J Neurophysiol 72:1634–1653

Grüsser OJ, Pause M, Schreiter U (1990a) Localization and responses of neurons in the parieto-insular vestibular cortex of the awake monkeys (*Macaca fascicularis*). J Physiol 430:537–557

Grüsser OJ, Pause M, Schreiter U (1990b) Vestibular neurons in the parieto-insular cortex of monkeys (*Macaca fascicularis*): visual and neck receptor responses. J Physiol 430:559–583

Guldin WO, Grüsser O-J (1996) The anatomy of the vestibular cortices of primates. In: Collard M, Jeannerod M, Christen Y (eds) The vestibular cortex. Editions IRVINN, Paris, pp 17–26

Guldin WO, Grüsser O-J (1998) Is there a vestibular cortex? Trends Neurosci 21:254–259

Heide W, Binkofski F, Seitz RJ, Posse S, Nitschke MF, Freund HJ, Kömpf D (2001) Activation of frontoparietal cortices during memorized triple-step sequences of saccadic eye movements: an fMRI study. Eur J Neurosci 13:1177–1189

Hoffmann KP, Distler C, Erickson R (1991) Functional projections from striate cortex and superior temporal sulcus to the nucleus of the optic tract (NOT) and dorsal terminal nucleus of the accessory optic tract (DTN) of Macaque monkeys. J Comp Neurol 313:707–724

Holstege G, Collewijn H (1982) The efferent connections of the nucleus of the optic tract and the superior colliculus in the rabbit. J Comp Neurol 209:139–175

Hutchinson M, Schiffer W, Joseffer S, Liu A, Schlosser R, Dikshit S, Goldberg E, Brodie JD (1999) Task-specific deactivation patterns in functional magnetic resonance imaging. Magn Reson Imaging 17:1427–1436

Ilg UJ (1997) Slow eye movements. Prog Neurobiol 53:293–329

Kawano K, Sasaki M, Yamashita M (1980) Vestibular input to visual tracking neurons in the posterior parietal association cortex of the monkey. Neurosci Lett 17:55–60

Kleinschmidt A, Thilo KV, Büchel C, Gresty MA, Bronstein AM, Frackowiak RSJ (2002) Neural correlates of visual-motion perception as object- or self-motion. Neuroimage 16:873–882

Leigh RJ, Zee DS (1999) The neurology of eye movements, 3rd edn. Oxford University Press, New York

Lobel E, Kleine JF, Le Bihan D, Leroy-Willig A, Berthoz A (1998) Functional MRI of galvanic vestibular stimulation. J Neurophysiol 80:2699–2709

Luna B, Thulborn KR, Strojwas MH, McCurtain BJ, Berman RA, Genovese CR, Sweeney JA (1998) Dorsal cortical regions subserving visually guided saccades in humans: an fMRI study. Cereb Cortex 8:40–47

Lynch JC, McLaren JW (1983) Optokinetic nystagmus deficits following parieto-occipital cortex lesions in monkeys. Exp Brain Res 49:125–130

Müri RM, Iba-Zizen MT, Derosier C, Cabanis EA, Pierrot-Deseilligny C (1996) Location of the human posterior eye field with functional magnetic resonance imaging. J Neurol Neurosurg Psychiatry 60:445–448

Naidich TP, Brightbill TC (1996) Systems for localizing frontoparietal gyri and sulci on axial CT and MRI. Int J Neuroradiol 2:313–338

Naidich TP, Valavanis AG, Kubik A (1995) Anatomic relationships along the low-middle convexity. I. Normal specimens and magnetic resonance imaging. Neurosurgery 36:517–532

Paus T (1996) Location and function of the human frontal eye-field: a selective review. Neuropsychologica 34:475–483

Petit L, Haxby JV (1999) Functional anatomy of pursuit eye movements in humans as revealed by fMRI. J Neurophysiol 81:463–471

Petit L, Clark VP, Ingeholm J, Haxby JV (1997) Dissociation of saccade-related and pursuit-related activation in human frontal eye fields as revealed by fMRI. J Neurophysiol 77:3386–3390

Rauch SL, Whalen PJ, Curran T, McInerney S, Heckers S, Savage C (1998) Thalamic deactivation during early implicit sequence learning: a functional MRI study. Neuroreport 9:865–870

Stephan KM, Schüller M, Höflich P, Knorr U, Binkofski F, Seitz RJ (1997) Normalization into Talairach space: variability of reference coordinates (abstract). Neuroimage 5:416

Sunaert S, Van Hecke P, Marchal G, Orban GA (1999) Motion-responsive regions of the human brain. Exp Brain Res 127:355–370

Talairach J, Tournoux P (1988) Co-planar stereotaxic atlas of the human brain. Thieme, Stuttgart

Tian JR, Lynch JC (1996a) Functionally defined smooth and saccadic eye movement subregions in the frontal eye field of *Cebus* monkeys. J Neurophysiol 76:2740–2753

Tian JR, Lynch JC (1996b) Corticocortical input to the smooth and saccadic eye movement subregions of the frontal eye field in *Cebus* monkeys. J Neurophysiol 76:2754–2771

Ventre J (1985) Cortical control of oculomotor functions. I. Optokinetic nystagmus. Behav Brain Res 15:211–226

Vitte E, Derosier C, Hasboun D, Caritu Y, Berthoz A (1996) Activation of the hippocampal formation by vestibular stimulation: an fMRI study. Exp Brain Res 112:523–526

Waespe W, Henn V (1977) Vestibular nuclei activity during optokinetic after-nystagmus (OKAN) in the alert monkey. Exp Brain Res 30:323–330

Waespe W, Henn V (1987) Gaze stabilisation in the primate. The interaction of the vestibulo-ocular reflex, optokinetic nystagmus, and smooth pursuit. Rev Physiol Biochem Pharmacol 106:37–125

Wenzel R, Bartenstein P, Dieterich M, Danek A, Weindl A, Minoshima S, et al (1996) Deactivation of human visual cortex during involuntary ocular oscillations: a PET activation study. Brain 119:101–110

Worsley KJ, Friston KJ (1995) Analysis of fMRI time-series revisited-again (comment). Neuroimage 2:173–181

Yousry TA, Fesl G, Büttner A, Noachtar S, Schmid DU, Peraud A, Winkler P (1997) Heschl's gyrus: anatomic description and methods of identification in MRI. Int J Neuroradiol 3:2–12

Zeki S, Watson JDG, Lueck CJ, Friston KJ, Kennard C, Frackowiak RSJ (1991) A direct demonstration of functional specialization in human visual cortex. J Neurosci 11:641–649